Br J Dermatol 2023; **00**:1–12
https://doi.org/10.1093/bjd/ljad095
Advance access publication date: 27 March 2023

BJD
British Journal of Dermatology
Translational Research

Chronic activation of Toll-like receptor 2 induces an ichthyotic skin phenotype

Hephzi Tagoe[1,2] Sakinah Hassan,[1,2] Emily Bliss,[3] Gehad Youssef,[1,2] Wendy Heywood,[3] Kevin Mills,[3] John I. Harper[2,4] and Ryan F.L. O'Shaughnessy[1]

[1]Centre for Cell Biology and Cutaneous Research, Queen Mary University of London, London, UK
[2]Livingstone Skin Research Centre
[3]Department of Genetics and Genomic Medicine
[4]Department of Immunobiology and Dermatology, UCL Great Ormond Street Institute of Child Health, London, UK

Correspondence Ryan O'Shaughnessy. Email: r.f.l.oshaughnessy@qmul.ac.uk

J.I.H. is deceased.

Abstract

Background Ichthyosis defines a group of chronic conditions that manifest phenotypically as a thick layer of scales, often affecting the entire skin. While the gene mutations that lead to ichthyosis are well documented, the actual signalling mechanisms that lead to scaling are poorly characterized; however, recent publications suggest that common mechanisms are active in ichthyotic tissue and in analogous models of ichthyosis.

Objectives To determine common mechanisms of hyperkeratosis that may be easily targeted with small-molecule inhibitors.

Methods We combined gene expression analysis of gene-specific short hairpin RNA (shRNA) knockdowns in rat epidermal keratinocytes (REKs) of two genes mutated in autosomal recessive congenital ichthyosis (ARCI), *Tgm1* and *Alox12b*, and proteomic analysis of skin scale from patients with ARCI, as well as RNA sequencing data from rat epidermal keratinocytes treated with the Toll-like receptor 2 (TLR2) agonist Pam3CSK4.

Results We identified common activation of the TLR2 pathway. Exogenous TLR2 activation led to increased expression of important cornified envelope genes and, in organotypic culture, caused hyperkeratosis. Conversely, blockade of TLR2 signalling in keratinocytes from patients with ichthyosis and our shRNA models reduced the expression of keratin 1, a structural protein overexpressed in ichthyosis scale. A time course of TLR2 activation in REKs revealed that although there was rapid initial activation of innate immune pathways, this was rapidly superseded by widespread upregulation of epidermal differentiation-related proteins. Both nuclear factor kappa B phosphorylation and GATA3 upregulation was associated with this switch, and GATA3 overexpression was sufficient to increase keratin 1 expression.

Conclusions Taken together, these data define a dual role for TLR2 activation during epidermal barrier repair that may be a useful therapeutic modality in treating diseases of epidermal barrier dysfunction.

What is already known about this topic?

- Multiple genetic mutations are associated with severe ichthyosis.
- Little is known about common mechanisms that could be targeted to reduce scaling in ichthyosis.

What does this study add?

- We show that activation of Toll-like receptor 2 (TLR2) causes scaling in three-dimensional culture and increases the expression of known markers of scale.

What is the translational message?

- TLR2 blockade can reduce the expression of these markers and may be a useful therapeutic modality in treating scaling in ichthyosis.

Accepted: 18 March 2023

The ichthyoses are a family of Mendelian diseases of keratinization.[1,2] Patients with autosomal recessive congenital ichthyosis (ARCI) are the most severely affected. Most children with ARCI present as a collodion baby at birth;[3] afterward, thick scales appear on their skin. As a result of improvements in neonatal care, there is a minimal risk of perinatal death due to insensible water loss and infections; however, patients' skin remains abnormal throughout life, and is the principal phenotype in ARCI.

ARCI can be divided into disease classes defined by diagnostic criteria. Lamellar ichthyosis (LI) typically presents at birth with a collodion. After the collodion is shed, thick scaling is present without redness of the skin, while nonbullous ichthyosiform erythroderma (NBIE) has lighter scaling and presents with redness of skin – collodion is less common.[1,4] Approximately 30% of cases of ARCI are caused by mutations in *TGM1*;[5] *TGM1* mutations are only rarely associated with NBIE.[4] Mutations in *ALOX12B* and *ALOXE3* account for 14% of ARCI but are common in NBIE.[6,7] At least 10 different genes are mutated in ARCI;[8,9] they all encode genes important for the epidermal barrier.

The scaling typically seen in ARCI reflects a homeostatic response to chronic barrier dysfunction. The barrier function of grafted *Tgm1* or *Alox12b* knockout skin on immunocompromised mice was restored through hyperkeratosis and increased lipid production.[10,11] Understanding the gene expression changes underlying these responses is critical in finding therapies to reduce scaling. Oral retinoids are the primary treatment for these patients, and while they efficiently reduce patient scale, they are associated with serious side-effects.[12] Although gene-specific gene therapy and protein-replacement therapies are being developed,[13–15] mechanism-specific, generalized therapies to reduce scaling are still needed. We examined the effects of *Tgm1* and *Alox12b* short hairpin RNA (shRNA) knockdown in keratinocytes. While there were distinct differences between the two knockdowns, there were common gene expression changes between the two lines that may define a common pathway of hyperkeratosis and scaling in ARCI.[16,17]

Significant progress has been made in understanding the mechanisms underlying scaling in ARCI. In *Tgm1* and *Alox12b* shRNA knockdown rat epidermal keratinocytes (REKs), we identified increased interleukin (IL)-1α signalling and upregulation of mouse double minute 2 homolog (MDM2) as necessary for hyperkeratosis.[16,17] MDM2 upregulation increased keratin 1, but not keratin 10, and this was also seen in patient scale samples.[16,17] Full-thickness skin biopsies from patients with ichthyosis revealed a T helper (Th)17/interleukin (IL)-23/IL-36-related signature of upregulated genes in both the dermis and epidermis of patients.[18,19] Upregulation of these signature genes correlated with increased transepidermal water loss (TEWL).[20] *ABCA12* shRNA knockdown that phenocopied the severe ichthyosis, harlequin ichthyosis, caused upregulation of key innate immune mediators, such as STAT1, the IL-36 family of cytokines and nitric oxide synthase 2.[21] These data strongly implicate innate immune pathways in ARCI.

Understanding the key keratinocyte-mediated mechanisms underlying altered innate immune signalling and scaling in these patients would allow for the identification of new therapeutic targets and discovery of molecular modulators of scaling. Using an integrated analysis of proteomics data from patient scales and datasets from our *in vitro* ARCI models, we identified upregulation of the Toll-like receptor 2 (TLR2) pathway. TLR2 activation caused scaling in REK organotypic models. TLR2 inhibition reduced expression of the terminal differentiation marker keratin 1 in ARCI models. RNA sequencing (RNAseq) analysis of a period of TLR2 activation showed a biphasic gene expression pattern, a short-term innate immune response and a longer-term GATA3-mediated hyperkeratotic response.

Materials and methods

Quadrupole time-of-flight mass spectrometry

These analyses have been described previously;[22] full details are provided in Appendix S1 (see Supporting Information).

Cell culture

Passage 20–30 REKs were cultured in Dulbecco's Modified Eagle Medium + 10% fetal bovine serum (Thermo Fisher Scientific, Waltham, MA, USA) and incubated at 37°C and 5% CO_2.[23] Organotypic culture was performed as described previously described:[24] 2×10^5 REKs were cultured in medium containing 100 mg mL^{-1} G418 on de-epidermized dermis made from cadaverous skin (Euro Skin Bank, Beverwijk, the Netherlands) in a metal ring until confluent. Cultures were raised to the air–liquid interface and cultured for a further 10 days. Cultures were processed for paraffin embedding by fixing in 4% paraformaldehyde. Sections of 5 mm were cut for immunofluorescence.

Human epidermal keratinocytes (HEKs; Thermo Fisher Scientific), and patient primary keratinocytes (passage five or less) were cultured in defined EpiLife™-supplemented medium (Thermo Fisher Scientific). Keratinocytes were differentiated by gradual calcium switch from 0.06 mmol L^{-1} to 2.4 mmol L^{-1} $CaCl_2$.[25] We used the following drugs: Pam3CSK4 10 μg mL^{-1} (Tocris Bioscience, Bristol, UK); CU-CPT-22 0.4 mmol L^{-1} (Sigma Aldrich, Irvine, UK); Etoposide 7.5 μg mL^{-1} (Sigma Aldrich); lipopolysaccharide 100 ng mL^{-1} (Sigma Aldrich); dithiothreitol 2.5 μL mL^{-1} (Invitrogen, Inchinnan, UK); and tunicamycin 50 ng mL^{-1} (Sigma Aldrich).

Alox12b and *Tgm1* shRNA knockdown in REKs using SureSilencing shRNA plasmids (QIAGEN, Hilden, Germany) has been described previously.[16,17] The human GATA3 construct for overexpression in REKs was obtained from OriGene (https://www.origene.com). All transfections were performed using lipofectamine 2000 (Thermo Fisher Scientific), according to manufacturer's instructions.

Immunofluorescence

Keratinocytes were fixed in 4% paraformaldehyde containing Triton-X-100 0.2% and blocked in phosphate buffered saline (PBS) containing Triton-X-100 0.2% and fish skin gelatin 0.2% (Sigma Aldrich). Primary and secondary antibodies were incubated in this blocking medium. Slides were mounted with 4′,6-diamidino-2-phenylindole-containing ProLong Gold™ (Thermo Fisher Scientific). Images were taken using a Leica DM4000 upright epifluorescence

microscope (Leica, Wetzlar, Germany). Antibody use is detailed in Appendix S1.

Western blotting

Proteins were extracted in total lysis buffer (sodium dodecyl sulfate 10%, β- mercaptoethanol 10 mmol L^{-1} Tris) at pH 7.5 and run on 10–20% TGX™ polyacrylamide gel (Bio-Rad, Hercules, CA, USA) and blotted onto Hybond™-N nitrocellulose filters (Amersham Biosciences, Little Chalfont, UK) and blocked in 5% milk powder in PBS containing 1× Tween-20 (Sigma Aldrich). The membrane incubated with the primary antibody at 4°C overnight. A secondary antibody was incubated for 60 min at room temperature. The membrane was developed on film (Amersham Biosciences) using enhanced chemiluminescence solution (Thermo Fisher Scientific). Antibody use is detailed in Appendix S1.

RNA sequencing analysis and downstream analyses

REKs were treated with Pam3CSK4 at 2, 6, 12 and 24 h, followed by RNA extraction and purification using the RNeasy kit (QIAGEN). Sample purity and concentration was determined using a NanoDrop (Thermo Fisher Scientific) and Bioanalyzer (Aglient, Santa Clara, CA, USA). Libraries were prepared using a mRNA library preparation kit (New England Biolabs, Ipswich, MA, USA) from 100 ng total RNA. Sequencing was done on a single lane of an Illumina NextSeq 500 (Illumina, San Diego, CA, USA) using a high-output kit with 75 base pair paired-end reads. Principal component analysis (PCA) was run on the gene expression data, followed by a two-way ANOVA to determine differentially expressed genes across all timepoints. Heat maps derived from these data and previous data were made using Morpheus (https://software.broadinstitute.org/morpheus).[16,17] STRING analysis (https://string-db.org) was performed using the full string network with a minimum confidence of 0.400 for positive evidence of association. Gene Ontology (GO) analyses were performed using DAVID (https://david.ncifcrf.gov).[26,27] Mapping of rat gene expression data to human promoter binding was performed with Enrichr (https://maayanlab.cloud/Enrichr/).[28]

Consent for tissue samples

Skin scale was obtained with consent from the patients' families at Great Ormond Street Hospital for Children, London, UK (REC 08/H0713/123). LI and NBIE keratinocytes were obtained from skin biopsies taken with consent at the Royal London Hospital.

Statistical and image analysis

All data analysed were based on mean values. Western blots were analysed with ImageJ (National Institutes of Health, Bethesda, MD, USA). A Student's *t*-test, ANOVA and post-hoc testing were used to assess the statistical significance between the treated and untreated samples. Gene expression changes were analysed using a two-tailed Student's *t*-test. RNAseq data were analysed by PCA and two-way ANOVA, and cell staining intensity was quantified in ImageJ.

Results

Combining proteomic and gene expression data revealed an upregulated SUMO1/Toll-like receptor 2/GATA3 axis in autosomal recessive congenital ichthyosis

To identify changes in expression in innate immune pathways, we combined the genes that were commonly differentially regulated in *Tgm1* and *Alox12b* shRNA knockdown REKs, a spontaneously transformed rat keratinocyte line that can fully differentiate in culture,[23] with mass spectrometry (MS) data comparing scale from four patients with ARCI of unknown genetic background and eight normal controls. We used REKs to investigate a wide variety of terminal differentiation phenomena and signalling pathways, with little or no differences between human and rat, and no differences in epidermal terminal differentiation, in submerged or organotypic culture.[16,17,29]

We identified 20 upregulated and 18 downregulated proteins by at least 1.5-fold in two or more patient samples (Figure 1a, b; Table S1, see Supporting Information). The most highly upregulated proteins were cathepsin D, apolipoprotein A1 and the SUMO ligase RANBP2. There was over-representation of proteins involved in the formation of the cornified envelope, keratinization, SUMOylation and TLR signalling (Figure 1c). As only a subset of proteins is typically detectable by MS of cornified envelopes,[22,30,31] we combined these data with our previous gene expression analyses of *Tgm1* and *Alox12b* shRNA knockdowns and identified a large protein–protein interaction network with a connection between RANBP2, SUMO1 and GATA3 (Figure 1d). We confirmed SUMO1 upregulation in our shRNA knockdown ARCI models (Figure 1e)[17] by immunofluorescence and Western blot (Figure 1f, g); we also identified increased SUMOylated proteins (Figure 1h).

Toll-like receptor 2 activation induced hyperkeratosis in organotypic culture

Based on the potential functional interaction between SUMO1 and TLR2, we tested the hypothesis that TLR2 activation induces Sumo expression by treating REKs with either lipopolysaccharide (LPS), which activates TLR4, or the synthetic ligand Pam3CSK4, which activates TLR2 for 24 h (Figure 2a). Sumo1 was upregulated only after Pam3CSK4 treatment. Testing different stressors indicated that Sumo1 upregulation occurred only with Pam3CSK4 treatment (Figure S1a; see Supporting Information). Increased keratin 1 expression, without concomitant expression of keratin 10, and upregulation of Il1a was only observed with LPS or Pam3CSK4 treatment (Figure S1b, c).

TLR2 signalling was upregulated in *Tgm1* and *Alox12b* shRNA knockdown REKs. While *Tlr2* mRNA expression was not significantly increased (Figure S2; see Supporting Information), TLR2 protein levels were increased in the shRNA knockdown lines (Figure 2b). There was also increased phosphorylation of the p65 subunit of nuclear factor kappa B (NFκB), consistent with our previous finding of increased nuclear localization of p65 in *Tgm1* shRNA knockdown organotypic cultures.[16] TLR2 activation by Pam3CSK4 caused p65 phosphorylation without Iκbα degradation (Figure 2b). Despite this, nuclear localization of

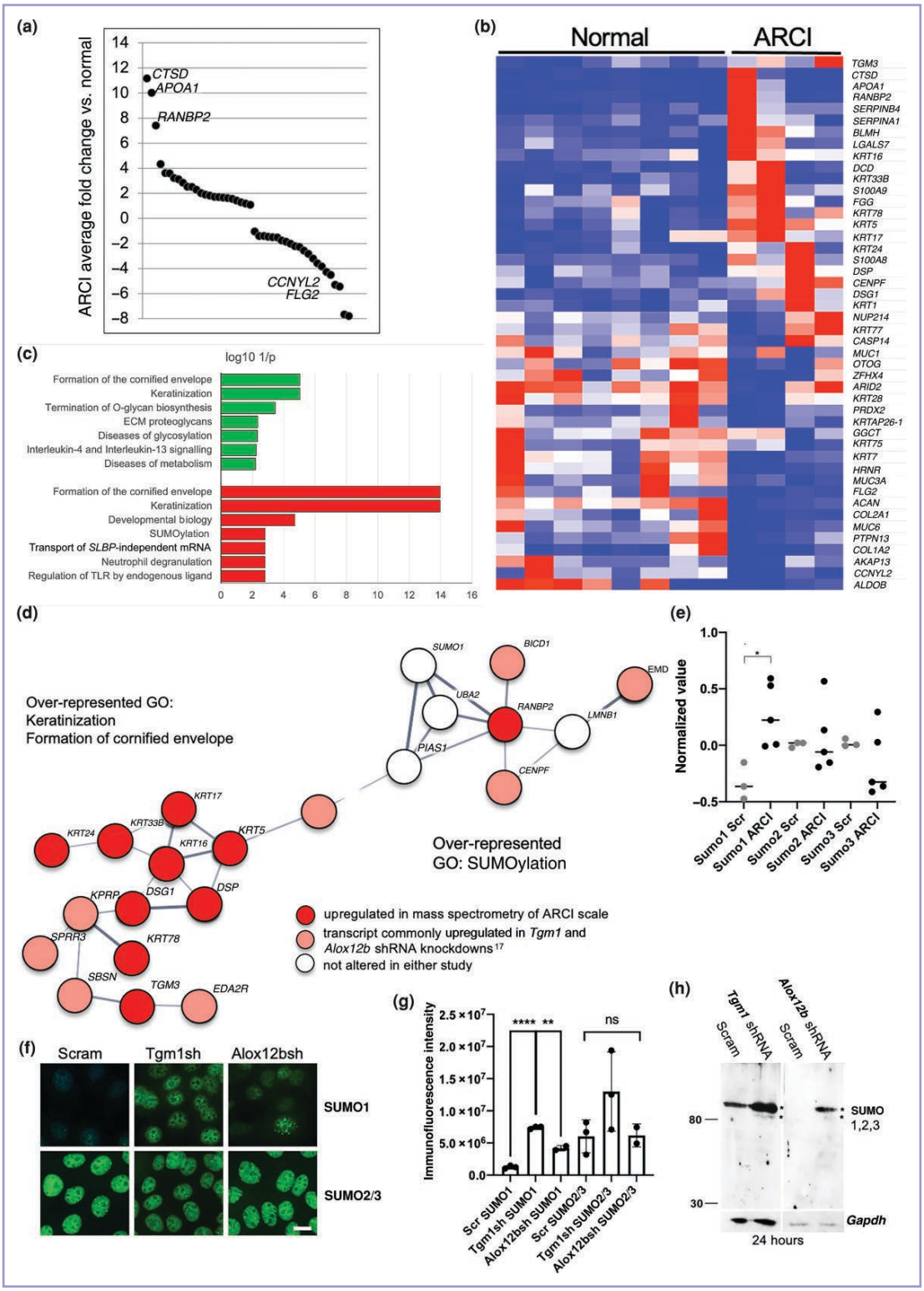

Figure 1 Combining proteomic and gene expression data revealed an upregulated SUMO1/Toll-like receptor 2 (TLR2)/GATA3 axis in autosomal recessive congenital ichthyosis (ARCI). (a) Average fold-change in protein expression from protein mass spectrometry data from ARCI patient scale ($n=4$) vs. normal skin ($n=8$). (b) Heat map of the data in (a); red indicates the maximum values and blue the minimum value for each row. (c) Over-represented biological process gene ontologies for up- (red) and downregulated proteins (green). ECM, extracellular matrix. (d) STRING network analysis of combined overexpressed proteins in scale and genes that are differentially expressed in both *Tgm1* and *Alox12b* short hairpin RNA (shRNA) knockdown rat epidermal keratinocytes.[17] GO, Gene Ontology. (e) Expression of each of the SUMO isoforms in control rat epidermal keratinocytes (Scr REKs; $n=3$) and in both the *Tgm1* and *Alox12b* shRNA knockdowns (ARCI, $n=5$ total), $P<0.05$ (Student's *t*-test). (f) Representative immunofluorescence of SUMO1 and SUMO2/3 in control REKs (Scr) and in both the *Tgm1* and *Alox12b* shRNA knockdowns (both $n=3$), bar = 10 mm. (g) SUMO1 and SUMO2/3 immunofluorescence intensity (**$P<0.005$, ****$P<0.00005$; ns, not significant). One-way ANOVA followed by post-hoc testing. (h) Western blot of a pan-SUMO antibody in control REKs (Scr) and in both the *Tgm1* and *Alox12b* shRNA knockdowns. *Over-represented SUMOylated protein species.

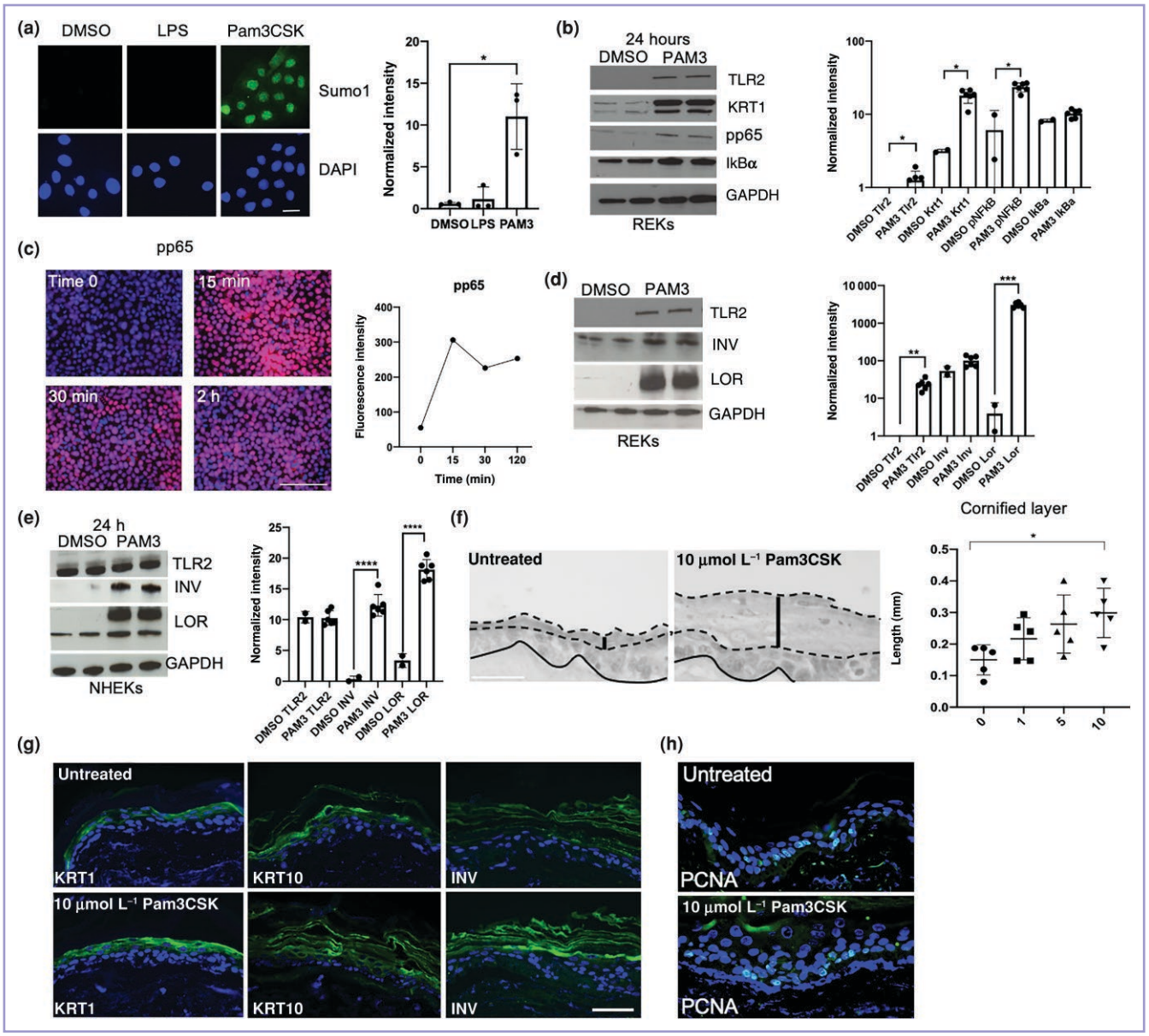

Figure 2 Activation of nuclear factor kappa B (NFκB) and epidermal terminal differentiation markers with Toll-like receptor 2 (TLR2) activation. (a) SUMO1 immunofluorescence in rat epidermal keratinocytes (REKs) treated with lipopolysaccharide (LPS), Pam3CSK4 or vehicle [dimethyl sulfoxide (DMSO)]. 4′,6-Diamidino-2-phenylindole was the nuclear counterstain. Graph shows normalized intensity ($n=3$). (b) Western blot of TLR2, keratin 1 (KRT1), phosphorylated-p65 (pp65) and IκBα in REKs treated with Pam3CSK4 (PAM3, $n=6$) or vehicle (DMSO, $n=2$). Glyceraldehyde 3-phosphate dehydrogenase (GAPDH) served as the loading control. Graph shows normalized intensity. (c) Phosphorylated p65 immunofluorescence in REKs over a 2 h period with the intensity graph on the right. (d, e) Western blots for TLR2, involucrin (INV) and loricrin (LOR) in Pam3CSK4- (PAM3, $n=6$) or vehicle-treated (DMSO, $n=2$) (d) REKs and (e) normal human epidermal keratinocytes (NHEKs). Graphs show normalized intensity. (f) Histology of REKs either treated or not with Pam3CSK4 from 5 days after raising to the air–liquid interface until day 10. The continuous line indicates the dermoepidermal junction and the dotted lines indicate the extent of the cornified layer. The thick bar indicates the thickness of the cornified layer. (f) Quantification of cornified layer thickness in Pam3CSK4-treated organotypic cultures measured at five sites over two different REK organotypic cultures in ImageJ. (g, h) Representative immunofluorescence of keratins 1 and 10 and (g) involucrin and (h) phosphorylated NFκB (pNFκB) in organotypic cultures treated with Pam3CSK ($n=2$). *$P<0.05$, **$P<0.005$, ***$P<0.0005$, ****$P<0.00005$ (one-way ANOVA followed by post-hoc testing); ns, not significant. Error bars show the SD of the mean. Bar in (a) = 10 mm; bar in (f, g) = 50 mm.

phosphorylated p65 occurred within 15 min of Pam3CSK4 treatment and was maintained for 2 h (Figure 2c). In both REKs and normal HEKs (NHEKs), 24 h of treatment with Pam3CSK4 upregulated key epidermal terminal differentiation markers keratin 1 (Figure 2c), loricrin and involucrin (Figure 2d, e). It was notable that while this was associated with an increase in TLR2 protein in REKs, in NHEKs, TLR2 was present before Pam3CSK4 treatment and did not change afterward. In organotypic culture, Pam3CSK4 induced a dose-dependent thickening of the cornified layer, without increased vital epidermal thickness (Figure 2f). Organotypic cultures treated with Pam3CSK4 showed keratin 1 and involucrin expression, while the expression of keratin 10 remained unchanged (Figure 2g). There was

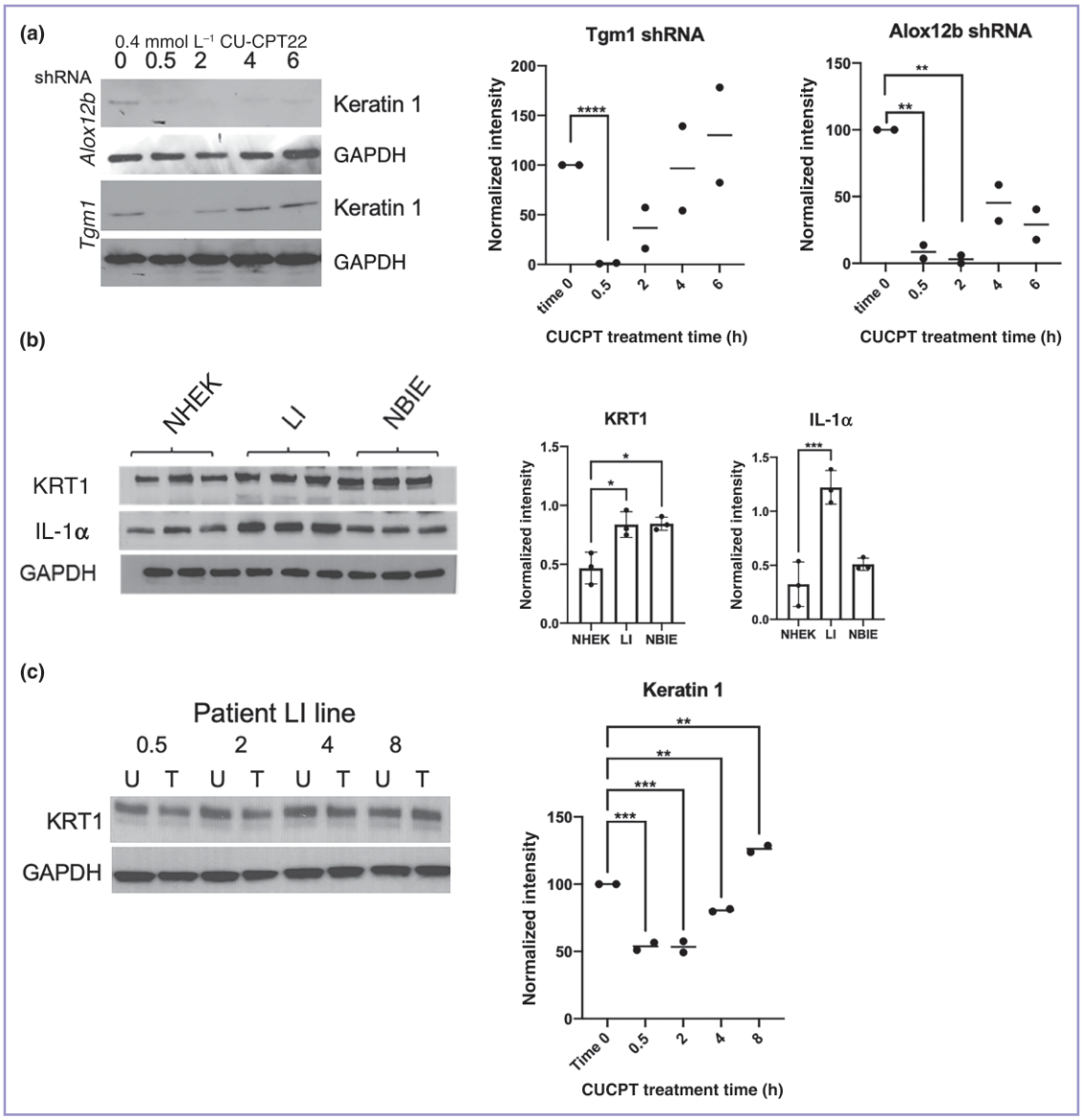

Figure 3 Toll-like receptor 2 (TLR2) inhibition reduced levels of keratin 1 in both autosomal recessive congenital ichthyosis (ARCI) models and in ARCI keratinocytes. (a) Western blot of keratin 1 in *Tgm1* and *Alox12b* short hairpin RNA (shRNA)-expressing rat epidermal keratinocytes (REKs) treated with the TLR2 inhibitor CU-CPT22 over 8 h. Glyceraldehyde 3-phosphate dehydrogenase (GAPDH) served as a loading control. Graphs show densitometry of two biological replicates, *Alox12b* and *Tgm1* shRNA-expressing REKs treated with CU-CPT22 showing the comparison as a percentage of the untreated time zero value. (b) Triplicate Western blots for keratin 1 (KRT1) and interleukin-1α (IL-1α) in primary keratinocytes from two patients with ARCI: one with lamellar ichthyosis (LI) and one with nonbullous ichthyosiform erythroderma (NBIE). GAPDH served as the loading control. NHEK, normalized human epidermal keratinocytes. Graphs show normalized densitometry of keratin 1 (KRT1) and IL-1α in both patient lines. (c) Representative Western blot ($n=2$) of KRT1 in the primary keratinocytes of a patient with LI treated once with CU-CPT22 at time 0 over 8 h. U, untreated; T, treated. Graph shows normalized intensity of Western blot. *$P<0.05$, **$P<0.005$, ***$P<0.0005$, ****$P<0.00005$ (one-way ANOVA with post-hoc testing).

no change in proliferating cell nuclear antigen, a marker of proliferating cells in these cultures (Figure 2h).

Toll-like receptor 2 inhibition reduced levels of keratin 1 in both autosomal recessive congenital ichthyosis models and in autosomal recessive congenital ichthyosis keratinocytes

CU-CPT22 is a selective inhibitor of TLR2.[32] CU-CPT22 treatment of *Tgm1* and *Alox12b* shRNA-expressing keratinocytes reduced keratin 1 expression over an 8 h period (Figure 3a), with a longer-lasting effect observed in *Alox12b* shRNA knockdowns. Treated non-genotyped ARCI primary keratinocytes from two patients diagnosed with LI and NBIE showed increased keratin 1 expression vs. normal keratinocytes, while IL-1α was increased only in LI keratinocytes (Figure 3b). CU-CPT22 treated caused a transient reduction of keratin 1 expression after a single treatment (Figure 3c).

RNA sequencing of rat epidermal keratinocytes treated with Pam3CSK4 indicated a biphasic pattern of nuclear factor kappa B activation

After a single Pam3CSK4 treatment, the expression of keratin 1 and IL1a was increased from 12 h and 2 h, respectively.

NFκB p65 showed both early and late increases in phosphorylation (Figure 4a), suggesting that multiple phases of gene expression change occurred, culminating in premature and increased expression of terminal differentiation markers. To examine this further, we performed RNAseq on REKs treated once with 10 mg mL^{-1} Pam3SCK over a 24 h period [Figure 4b, c; RPKM (reads per kb of transcript per million reads mapped) expression data are provided in Table S2; see Supporting Information]. In total, 1810 genes were significantly differentially expressed over this timescale (Figure 4b). Consistent with data from the ARCI shRNA lines, Pam3CSK4 treatment did not significantly increase *Tlr2* mRNA expression, although there was a transient increase in *Tlr4* at 2 h and a progressive decrease in *Tlr5* expression (Figure S3; see Supporting Information).

PCA showed a biphasic change in gene expression. Changes from 0 h to 2 h were seen in PC2, while changes in gene expression at 12 and 24 h were seen in PC1 (Figure 4c). We identified six different patterns of gene expression change in our RNAseq data [Figure 4d; Table S3 (see Supporting Information)] reflecting the dynamic changes in gene expression: cluster 1 was transiently overexpressed at the 2 h timepoint, cluster 2 was significantly downregulated from 12 to 24 h, cluster 3 was maximally expressed at 24 h, cluster 4 genes peaked at 6 h, cluster 5 gene expression increased progressively over the treatment period and cluster 6 gene expression fell progressively over the treatment period. GO analysis revealed that cluster 1 was associated with positive regulation of apoptosis, cluster 2 was associated with cell division, and cluster 3 was associated with keratinocyte differentiation and the formation of the cornified envelope, and included both keratin 1 and IL-1α. Cluster 4 was associated with proteolysis, cluster 5 with actin binding and cluster 6 with the nucleosome (Figure 4e). Further analysis of keratinocyte differentiation-associated genes revealed that while some genes, such as *Evpl* and *Cers3*, were prematurely induced compared to keratin 10, other important terminal differentiation-related keratin genes such as *Krt2* were not induced over the same timescale. Basal and simple keratins (5, 14 and 8) were transiently induced, suggesting that there was a hyperkeratosis-specific programme of terminal differentiation induced by Pam3CSK (Figure S4; see Supporting Information).

We analysed the signalling pathways upregulated in each cluster with Enrichr (Figure 4f). Tumour necrosis factor (TNF)-α/NFκB signalling was significantly increased in clusters 1 and 3, reflecting the biphasic activation discussed above. Cluster 2 was enriched in genes associated with aspects of the cell cycle, consistent with a switch to increased terminal differentiation. Clusters 4 and 5 were associated with the early oestrogen response. Cluster 6 was strongly associated with Ras signalling, again reflecting a switch from proliferation to differentiation. TNF-α/NFκB-related genes were different between clusters 1 and 3, with cluster 1 consisting of genes related to innate immunity and cytokine signalling, while cluster 3 consisted of genes involved in transcription, growth factor signalling and angiogenesis (Figure 4g). These data suggest that NFκB signalling plays two different roles during the time course of the response to TLR2 activation.

GATA3 upregulation increased keratin 1 expression downstream of Toll-like receptor 2 activation

To determine which of the genes controlled by TLR2 activation were involved in hyperkeratosis in ARCI, we compared the RNAseq gene expression data with our previous analysis of *Tgm1* and *Alox12b* shRNA knockdowns. Thirty-eight of 61 (62%) genes were coordinately differentially expressed in both analyses [Figure 5a (Table S4; see Supporting Information)].[17]

GATA3 was increased in both the *Tgm1* and *Alox12b* knockdown rat epidermal keratinocytes, with higher expression in *Alox12b* knockdown keratinocytes (Figure 5b). In the Pam3CSK4 RNAseq analysis, *Gata3* was in cluster 3; the genes increased maximally at 24 h. However, *Gata3* mRNA expression progressively increased during the whole treatment period, prior to the increase in keratin 1 (Figure 5c). GATA3 increased after 12–24 h of Pam3CSK4 treatment in both REKs and HEKs (Figure 5d, e). Genes with GATA3 binding promoters were significantly over-represented in cluster 3 genes (Figure S4a), and they were enriched for both genes involved in epidermal terminal differentiation and lipid synthesis (Figure S5b, c), suggesting that the upregulation of epidermal differentiation genes and lipid synthesis was potentially driven by the upregulation of GATA3. GATA3 increased in NBIE keratinocytes but not in LI keratinocytes (Figure 5f). Overexpression of GATA3 in REKs (Figure 5g, h) increased keratin 1 expression. However, treatment with Pam3CSK4 did not increase K1 further, suggesting that GATA3 was downstream of TLR2 activation, and potentially was a key downstream driver of the longer-term effects of TLR2 activation leading to hyperkeratosis.

Discussion

TLR signalling and SUMOylation is activated in ARCI models. TLR2 activation is necessary for hyperkeratosis and blockade of TLR2 signalling in ARCI models, and patient primary keratinocytes reduced the increased levels of keratin 1 seen in ARCI.[16,17] We show proof of principle that TLR2 blockade transiently reduced keratin 1 expression in patient keratinocytes. In HEK293 cells, CU-CPT22 treatment reduced nuclear NFκB at 20 min,[33] while in keratinocytes inoculated with *Propionibacterium acnes*, CU-CPT22 was still effective after 24 h.[34] This suggests that the effects of CU-CPT22 are either variable and context-dependent or that the TLR2–NFκB-mediated pathway that increased keratin 1 is different and responds differently to CU-CPT22. More investigation into both the stability of CU-CPT22 and the effects of treatment on a background of ARCI are required.

TLR2 upregulated SUMO1 in REKs. Typically, SUMO activation, and SUMOylation correlates with downregulation of the innate immune response.[35] SUMOylation increases during epidermal terminal differentiation,[36] and SUMOylated substrate proteins are concentrated in the upper epidermis, conferring a significant proportion of skin barrier function. Inhibition of SUMOylation prevented keratinocyte differentiation. This is consistent with increased SUMOylation associating with a protective prodifferentiation response

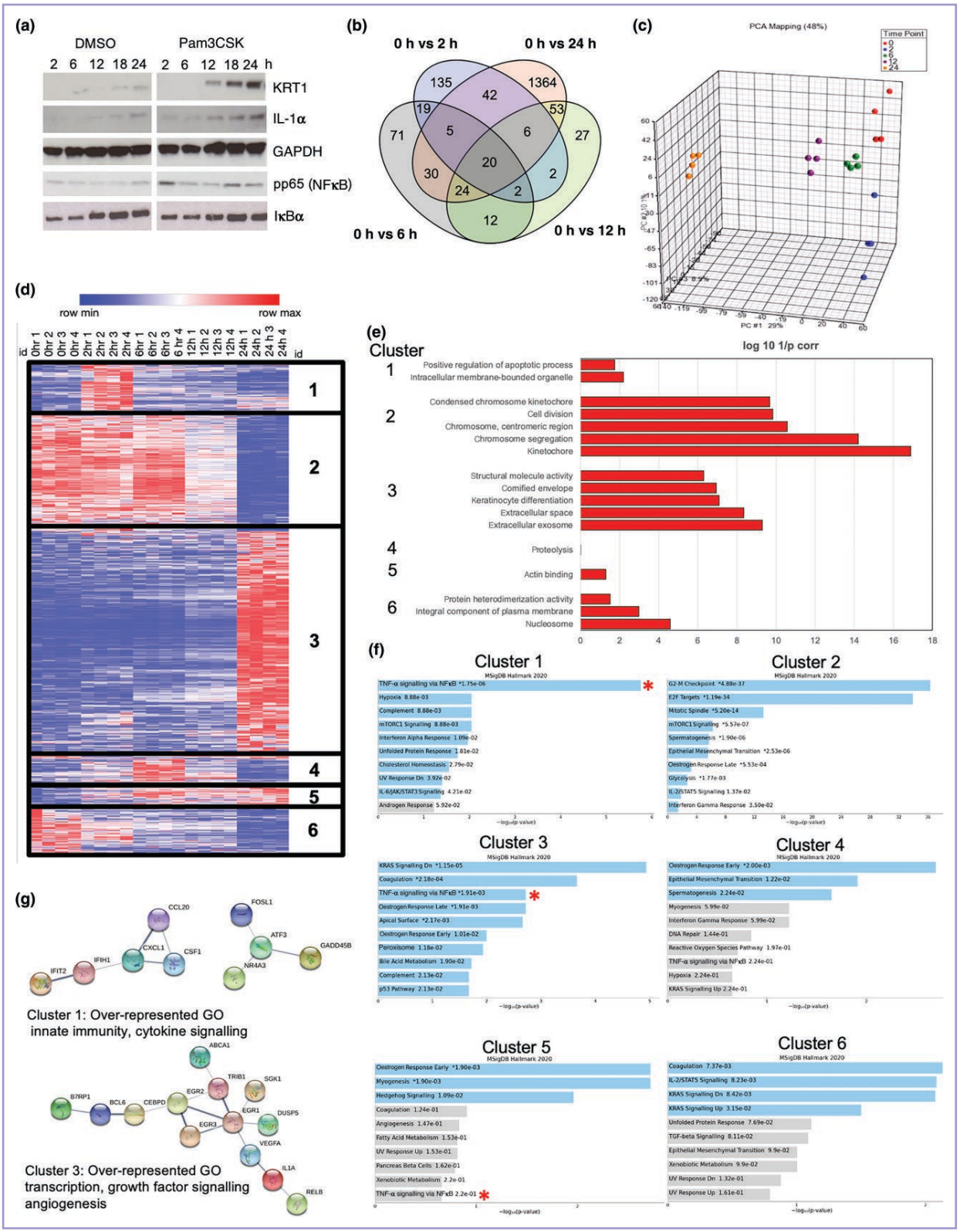

Figure 4 RNA sequencing (RNAseq) analysis and signalling pathway analysis of rat epidermal keratinocytes (REKs) treated with Pam3CSK4 indicated a biphasic pattern of nuclear factor kappa B (NFκB) activation. (a) Western blot of REKs treated with Pam3CSK4 or vehicle (dimethyl sulfoxide; DMSO) over a 24 h period ($n=2$). Glyceraldehyde 3-phosphate dehydrogenase (GAPDH) served as a loading control. KRT1, keratin 1; IL-1α, interleukin-1α; pp65, phosphorylated p65. (b) Venn diagram showing differentially expressed genes at different timepoints during the 24 h RNA sequencing experiment. (c) Graphical representation of principal component analysis showing the variation at both early and late timepoints ($n=4$ at each timepoint). (d) Heat map and cluster analysis of all differentially expressed genes in the RNAseq experiment. (e) Analysis of over-represented Gene Ontology (GO) groups in each of the clusters described in (d). (f) Enrichr analysis of signalling related genes in each of the clusters. Blue denotes significant over-representation after correction for multiple testing. The red asterisk indicates tumour necrosis factor (TNF)/NFκB signalling in the relevant clusters. (g) String analysis and GO analysis of the TNF/NFκB signalling genes in clusters 1 and 3.

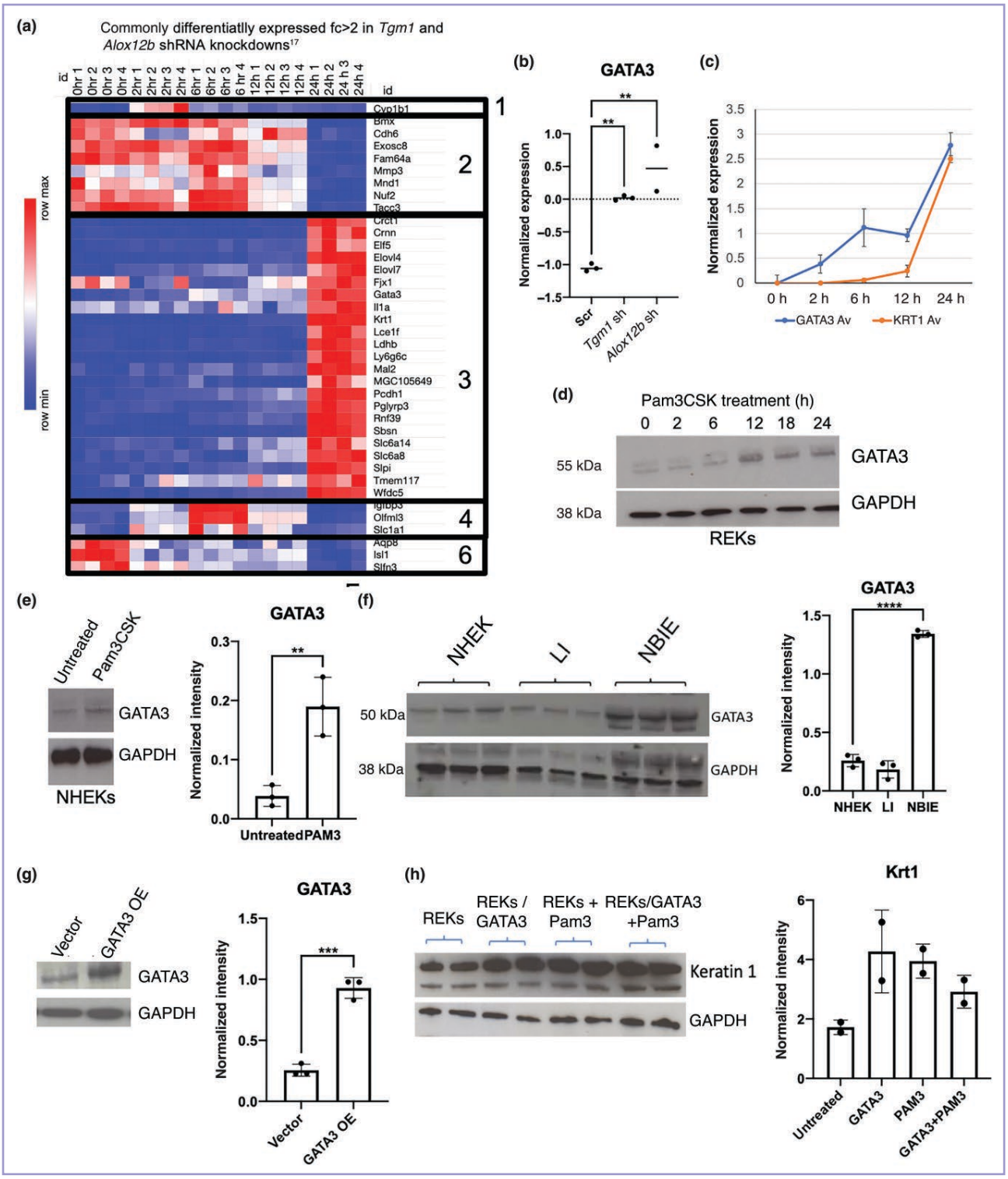

Figure 5 GATA3 upregulation increased keratin 1 expression downstream of Toll-like receptor activation. (a) Heat map of genes differentially expressed in both *Tgm1* and *Alox12b* short hairpin RNA (shRNA) knockdown rat epidermal keratinocytes (REKs)[17] and in the Pam3CSK4-treated REKs. Differentially expressed genes are mapped to each of the clusters identified in Figure 4 ($n=4$ at each timepoint). (b) Normalized Affymetrix signals of GATA3 in *Tgm1* ($n=3$) and *Alox12b* ($n=2$) shRNA knockdown and Scrambled (Scr) control samples ($n=3$). (c) Graph of normalized expression of GATA3 and keratin 1 (KRT1) across the 24 h period of Pam3CSK treatment. (d) Representative Western blot of GATA3 in REKs treated with Pam3CSK4 over a 24 h period. (e) Western blot of GATA3 in normal human epidermal keratinocytes (NHEKs) treated with Pam3CSK4 for 24 h; on the right is a graphical representation of normalized densitometry data ($n=3$). (f). Western blot of GATA3 in lamellar ichthyosis (LI) and nonbullous ichthyosiform erythroderma (NBIE) keratinocytes and normal controls (each $n=3$). Graph shows normalized intensity. (g) Western blot of GATA3 in GATA3 overexpressing REKs (GATA3 OE) vs. vector alone. Graph shows normalized densitometry data ($n=3$). (h) Western blot of duplicate REK cultures overexpressing GATA3, treated with Pam3CSK4 or overexpressing cells treated with Pam3CSK4 for KRT1 ($n=2$); glyceraldehyde 3-phosphate dehydrogenase (GAPDH) served as the loading control. Graph shows normalized intensity. Bars represent the SD. $^{**}P<0.005$, $^{***}P<0.0005$, $^{****}P<0.00005$, one-way ANOVA with post-hoc testing.

in individuals with ARCI. SUMOylation is known to control inflammation and antiviral responses during innate sensing, with SUMOylation blunting these responses in mice due to enhancer binding in proinflammatory genes.[37] Therefore, SUMOylation caused by impaired barrier function in ARCI may be required to direct the TLR2/NFκB response toward a barrier repair programme.

Activation of TLR2 leads to the upregulation of claudin, and loss of TLR2 correlates with increased TEWL.[38] Therefore, it is likely that the increased TLR2 signalling is a protective response to the defective barrier in ichthyosis. The increased thickness of the cornified layer in organotypic cultures treated with Pam3CSK4 supports this concept. TLR2 activation may rescue epidermal barrier function, in part, by the activation of tight junctions.[39] We have shown, via comprehensive RNAseq analysis, that the effects of TLR2 activation are wider ranging than their established role in classical innate immune activation. We have identified novel functions for TLR2 signalling in epidermal terminal differentiation and lipid synthesis, both of which are required for optimal barrier restoration in response to severe barrier defects in ARCI.

One difference between rats and humans is the different TLR2 expression changes in response to Pam3CSK4 treatment, and how this relates to differences in TLR2 expression and signalling in barrier disruption. TLR2 is constitutively expressed in human epidermis,[40] consistent with the data obtained from keratinocytes, and protein expression levels do not change in patients with barrier dysfunction.[41] However, in mouse skin, TLR2 protein levels are increased in response to barrier disruption, such as tape stripping;[42] however, the downstream effect (i.e. upregulation of terminal differentiation markers) remained the same. Therefore, TLR2 activation is directly linked to epidermal terminal differentiation.

We observed biphasic activation of NFκB signalling after Pam3CSK4 treatment. This is consistent with previous data that showed upregulation of nuclear p65 in *Tgm1* shRNA-expressing REK organotypic cultures.[16] Here we have shown that NFκB-related genes are markedly different in the 'early' and 'late' phase of the response to TLR2 activation. Our previous studies likely reflected the late stages of the TLR2 activation response, post-24 h. While NFκB signalling is required for the innate immune response, this was only apparent at early timepoints, while the second peak of NFκB signalling at 24 h was more clearly associated with a barrier protective response, including the expression of epidermal differentiation and lipid synthesis genes, and has also been seen in the flaky tail mouse – a model for ichthyosis vulgaris.[43] NFκB subunit deletion or inhibition can also result in skin hyperproliferation and inflammation.[44] Control of NFκB signalling is complex, involving both the pattern recognition receptors such as TLRs, signalling through Myd88 and the action of IκB kinase (IKK) degrading IκBα, which allows NFκB into the nucleus.[45] *Ikk2* knockout mice have impaired epidermal terminal differentiation during murine development.[46] Together, this implicates nuclear translocation of NFκB in response to TLR2 activation in activating epidermal terminal differentiation in response to the barrier dysfunction in ARCI.

GATA3 shRNA knockdown causes barrier impairment related to the loss of expression of lipid synthesis genes,[47] and *GATA3* overexpression increases the expression of keratinization genes such as loricrin and inhibits proliferation.[48–50] Upregulation of lipid synthesis genes and epidermal terminal differentiation-related genes occurred in both Pam3CSK4-treated REKs and NHEKs, and in our *Tgm1* and *Alox12b* shRNA knockdown REKs;[17] downregulation of cell cycling was seen specifically in the *Alox12b* shRNA knockdown keratinocytes.[17] *GATA3* methylation by the drug DZ2002 reduces psoriasis skin lesions.[51] *GATA3* is a p63 target gene and is involved in the upregulation of IKK-α, which is also involved in epidermal differentiation,[52] linking *GATA3* to the upregulation of the NFκB response in cluster 3 genes. Our data support a role for TLR2, NFκB signalling and GATA3 in establishing an altered epidermal differentiation programme in response to disrupted barrier function in ARCI. One outstanding issue that may have further therapeutic implications is that TLR2 signalling in our ARCI shRNA models is increased, suggesting that there is an endogenous ligand present in defective differentiated cells. Although outside of the scope of this study, heat shock proteins HSP60 and HSP70 are abundant in differentiating keratinocytes and activate TLR2 signalling.[53,54] Understanding the extracellular milieu in barrier-defective skin may reveal further therapeutic targets to reduce hyperkeratosis induced by TLR2 activation.

Acknowledgements

We thank the QMUL Genome Centre for the RNA sequencing and subsequent analyses. R.F.L.O'S., J.I.H. and K.M. conceived the study. R.F.L.O'S., H.T. and S.H. designed experiments. H.T., S.H. and W.H. performed experiments and interpreted data. The manuscript was written by R.F.L.O'S., K.M. and H.T., and was contributed to by all authors.

Funding sources

This work was supported by the British Skin Foundation, the Foundation for Ichthyosis and Related Skin Types (F.I.R.S.T.), and the Great Ormond Street Hospital Charity. The funders were not involved in study design, data collection and analysis, manuscript preparation or publication decisions.

Conflicts of interest

The authors declare they have no conflicts of interest.

Data availability

The data underlying this article will be shared on reasonable request to the corresponding author.

Ethics statement

Skin scale was obtained with consent from families at Great Ormond Street Hospital for Children, London (REC 08/

H0713/123). Lamellar ichthyosis and nonbullous ichthyosiform erythroderma keratinocytes were obtained from skin biopsies taken with consent at the Royal London Hospital.

Supporting Information

Additional Supporting Information may be found in the online version of this article at the publisher's website.

References

1 Oji V, Tadini G, Akiyama M *et al.* Revised nomenclature and classification of inherited ichthyoses: results of the First Ichthyosis Consensus Conference in Sorèze 2009. *J Am Acad Dermatol* 2010; **63**:607–41.
2 Takeichi T, Akiyama M. Inherited ichthyosis: non-syndromic forms. *J Dermatol* 2016; **43**:242–51.
3 Dyer JA, Spraker M, Williams M. Care of the newborn with ichthyosis. *Dermatol Ther* 2013; **26**:1–15.
4 Vahlquist A, Bygum A, Gånemo A *et al.* Genotypic and clinical spectrum of self-improving collodion ichthyosis: *ALOX12B*, *ALOXE3*, and *TGM1* mutations in Scandinavian patients. *J Invest Dermatol* 2010; **130**:438–43.
5 Russell LJ, DiGiovanna JJ, Rogers GR *et al.* Mutations in the gene for transglutaminase 1 in autosomal recessive lamellar ichthyosis. *Nat Genet* 1995; **9**:279–83.
6 Hotz A, Kopp J, Bourrat E *et al.* Meta-analysis of mutations in *ALOX12B* or *ALOXE3* identified in a large cohort of 224 patients. *Genes (Basel)* 2021; **12**:80.
7 Jobard F, Lefèvre C, Karaduman A *et al.* Lipoxygenase-3 (*ALOXE3*) and (R)-lipoxygenase (*ALOX12B*) are mutated in non-bullous congenital ichthyosiform erythroderma (NCIE) linked to chromosome 17p13.1. *Hum Mol Genet* 2002; **11**:107–13.
8 Uitto J, Youssefian L, Saeidian AH, Vahidnezhad H. Molecular genetics of keratinization disorders – what's new about ichthyosis. *Acta Derm Venereol* 2020; **100**:adv00095.
9 Youssefian L, Vahidnezhad H, Saeidian AH *et al.* Autosomal recessive congenital ichthyosis: genomic landscape and phenotypic spectrum in a cohort of 125 consanguineous families. *Hum Mutat* 2019; **40**:288–98.
10 Kuramoto N, Takizawa T, Takizawa T *et al.* Development of ichthyosiform skin compensates for defective permeability barrier function in mice lacking transglutaminase 1. *J Clin Invest* 2002; **109**:243–50.
11 de Juanes S, Epp N, Latzko S *et al.* Development of an ichthyosiform phenotype in Alox12b-deficient mouse skin transplants. *J Invest Dermatol* 2009; **129**:1429–36.
12 Rood MJ, Lavrijsen SP, Huizinga TW. Acitretin-related ossification. *J Rheumatol* 2007; **34**:837–8.
13 Choate KA, Medalie DA, Morgan JR, Khavari PA. Corrective gene transfer in the human skin disorder lamellar ichthyosis. *Nat Med* 1996; **2**:1263–7.
14 Aufenvenne K, Larcher F, Hausser I *et al.* Topical enzyme-replacement therapy restores transglutaminase 1 activity and corrects architecture of transglutaminase-1-deficient skin grafts. *Am J Hum Genet* 2013; **93**:620–30.
15 Plank R, Yealland G, Miceli E *et al.* Transglutaminase 1 replacement therapy successfully mitigates the autosomal recessive congenital ichthyosis phenotype in full-thickness skin disease equivalents. *J Invest Dermatol* 2019; **139**:1191–5.
16 O'Shaughnessy RF, Choudhary I, Harper JI. Interleukin-1 alpha blockade prevents hyperkeratosis in an *in vitro* model of lamellar ichthyosis. *Hum Mol Genet* 2010; **19**:2594–605.
17 Youssef G, Ono M, Brown SJ *et al.* Identifying a hyperkeratosis signature in autosomal recessive congenital ichthyosis: Mdm2 inhibition prevents hyperkeratosis in a rat ARCI model. *J Invest Dermatol* 2014; **134**:858–61.
18 Malik K, He H, Huynh TN *et al.* Ichthyosis molecular fingerprinting shows profound TH17 skewing and a unique barrier genomic signature. *J Allergy Clin Immunol* 2019; **143**:604–18.
19 Paller AS, Renert-Yuval Y, Suprun M *et al.* An IL-17-dominant immune profile is shared across the major orphan forms of ichthyosis. *J Allergy Clin Immunol* 2017; **139**:152–65.
20 Brunner PM, Israel A, Zhang N *et al.* Early-onset pediatric atopic dermatitis is characterized by TH2/TH17/TH22-centered inflammation and lipid alterations. *J Allergy Clin Immunol* 2018; **141**:2094–106.
21 Enjalbert F, Dewan P, Caley MP *et al.* 3D model of harlequin ichthyosis reveals inflammatory therapeutic targets. *J Clin Invest* 2020; **130**:4798–810.
22 Bennett K, Callard R, Heywood W *et al.* New role for LEKTI in skin barrier formation: label-free quantitative proteomic identification of caspase 14 as a novel target for the protease inhibitor LEKTI. *J Proteome Res* 2010; **9**:4289–94.
23 Baden HP, Kubilus J. The growth and differentiation of cultured newborn rat keratinocytes. *J Invest Dermatol* 1983; **80**:124–30.
24 O'Shaughnessy RF, Welti JC, Cooke JC *et al.* AKT-dependent HspB1 (Hsp27) activity in epidermal differentiation. *J Biol Chem* 2007; **282**:17297–305.
25 Bikle DD, Xie Z, Tu CL. Calcium regulation of keratinocyte differentiation. *Expert Rev Endocrinol Metab* 2012; **7**:461–72.
26 Huang DW, Sherman BT, Lempicki RA. Bioinformatics enrichment tools: paths toward the comprehensive functional analysis of large gene lists. *Nucleic Acids Res* 2009; **37**:1–13.
27 Huang DW, Sherman BT, Lempicki RA. Systematic and integrative analysis of large gene lists using DAVID Bioinformatics Resources. *Nature Protoc* 2009; **4**:44–57.
28 Chen EY, Tan CM, Kou Y *et al.* Enrichr: interactive and collaborative HTML5 gene list enrichment analysis tool. *BMC Bioinformatics* 2013; **128**:128.
29 Rogerson C, Wotherspoon DJ, Tommasi C *et al.* Akt1-associated actomyosin remodelling is required for nuclear lamina dispersal and nuclear shrinkage in epidermal terminal differentiation. *Cell Death Differ* 2021; **28**:1849–64.
30 Karim N, Phinney BS, Salemi M *et al.* Human stratum corneum proteomics reveals cross-linking of a broad spectrum of proteins in cornified envelopes. *Exp Dermatol* 2019; **28**:618–22.
31 Winget JM, Finlay D, Mills KJ *et al.* Quantitative proteomic analysis of stratum corneum dysfunction in adult chronic atopic dermatitis. *J Invest Dermatol* 2016; **136**:1732–5.
32 Cheng K, Wang X, Zhang S, Yin H. Discovery of small-molecule inhibitors of the TLR1/TLR2 complex. *Angew Chem Int Ed Engl* 2012. **51**:12246–9.
33 Daniele SG, Béraud D, Davenport C *et al.* Activation of MyD88-dependent TLR1/2 signaling by misfolded α-synuclein, a protein linked to neurodegenerative disorders. *Sci Signal* 2015; **8**:ra45.
34 Su Q, Grabowski M, Weindl G. Recognition of *Propionibacterium acnes* by human TLR2 heterodimers. *Int J Med Microbiol* 2017; **307**:108–12.
35 Hanke NT, LaCasse CJ, Larmonier CB *et al.* PIAS1 and STAT-3 impair the tumoricidal potential of IFN-γ-stimulated mouse dendritic cells generated with IL-15. *Eur J Immunol* 2014; **44**:2489–99.
36 Deyrieux AF, Rosas-Acosta G, Ozbun MA, Wilson VG. Sumoylation dynamics during keratinocyte differentiation. *J Cell Sci* 2007; **120**:125–36.
37 Decque A, Joffre O, Magalhaes JG *et al.* Sumoylation coordinates the repression of inflammatory and anti-viral gene expression programs during innate sensing. *Nat Immunol* 2016; **17**:140–9.
38 Kuo IH, Carpenter-Mendini A, Yoshida T. Activation of epidermal toll-like receptor 2 enhances tight junction function: implications

for atopic dermatitis and skin barrier repair. *J Invest Dermatol* 2013; **133**:988–98.
39 Yuki T, Yoshida H, Akazawa Y *et al.* Activation of TLR2 enhances tight junction barrier in epidermal keratinocytes. *J Immunol* 2011; **187**:3230–7.
40 Panzer R, Blobel C, Fölster-Holst R, Proksch E. TLR2 and TLR4 expression in atopic dermatitis, contact dermatitis and psoriasis. *Exp Dermatol* 2014; **23**:364–6.
41 Donetti E, Cornaghi L, Arnaboldi F *et al.* Epidermal barrier reaction to an *in vitro* psoriatic microenvironment. *Exp Cell Res* 2017; **360**:180–8.
42 Jin H, Kumar L, Mathias C, *et al*. Toll-like receptor 2 is important for the T(H)1 response to cutaneous sensitization. *J Allergy Clin Immunol* 2009; **123**:875–82.
43 Kypriotou M, Boéchat C, Huber M, Hohl D. Spontaneous atopic dermatitis-like symptoms in a/a ma ft/ma ft/J flaky tail mice appear early after birth. *PLoS One* 2013; **8**:e67869.
44 Kumari S, Van TM, Preukschat D *et al.* NF-κB inhibition in keratinocytes causes RIPK1-mediated necroptosis and skin inflammation. *Life Sci Alliance* 2021; **4**:e202000956.
45 Descargues P, Sil AK, Karin M. IKKalpha, a critical regulator of epidermal differentiation and a suppressor of skin cancer. *EMBO J* 2008; **27**:2639–47.
46 Pasparakis M, Courtois G, Hafner M *et al.* TNF-mediated inflammatory skin disease in mice with epidermis-specific deletion of IKK2. *Nature* 2002; **417**:861–6.
47 de Guzman Strong C, Wertz PW *et al.* Lipid defect underlies selective skin barrier impairment of an epidermal-specific deletion of Gata-3. *J Cell Biol* 2006; **175**:661–70.
48 Kawachi Y, Ishitsuka Y, Maruyama H *et al.* GATA-3 regulates differentiation-specific loricrin gene expression in keratinocytes. *Exp Dermatol* 2012; **21**:859–64.
49 Masse I, Barbollat-Boutrand L, Kharbili ME *et al.* GATA3 inhibits proliferation and induces expression of both early and late differentiation markers in keratinocytes of the human epidermis. *Arch Dermatol Res* 2014; **306**:201–8.
50 Zeitvogel J, Jokmin N, Rieker S *et al.* GATA3 regulates FLG and FLG2 expression in human primary keratinocytes. *Sci Rep* 2017; **7**:11847.
51 Chen L, Lin Z, Liu Y *et al.* DZ2002 alleviates psoriasis-like skin lesions via differentially regulating methylation of GATA3 and LCN2 promoters. *Int Immunopharmacol* 2021; **91**:107334.
52 Candi E, Terrinoni A, Rufini A *et al.* p63 is upstream of IKK alpha in epidermal development. *J Cell Sci* 2006; **119**:4617–22.
53 Vabulas RM, Ahmad-Nejad P, Ghose S *et al.* HSP70 as endogenous stimulus of the Toll/interleukin-1 receptor signal pathway. *J Biol Chem* 2002; **277**:15107–12.
54 Habich C, Baumgart K, Kolb H, Burkart V. The receptor for heat shock protein 60 on macrophages is saturable, specific, and distinct from receptors for other heat shock proteins. *J Immunol* 2002; **168**:569–76.

Bimzelx® ▼
(bimekizumab)

THIS ADVERT CONTAINS PROMOTIONAL CONTENT FROM UCB AND IS INTENDED FOR HCPS IN THE UK

THE OPPORTUNITY FOR COMPLETE, FAST AND LASTING SKIN CLEARANCE[1,2]

- **In phase III studies BIMZELX demonstrated superiority vs ustekinumab (BE VIVID; p<0.0001), placebo (BE READY; p<0.0001) and adalimumab (BE SURE; p< 0.001) in achieving the co-primary endpoints PASI 90 and IGA 0/1 at week 16 with 85% (273/321), 90.8% (317/349) and 86.2% (275/319) of patients achieving PASI 90 at Week 16. At Week 4, 76.9% (247/321), 75.9% (265/349) and 76.5% (244/319) of patients achieved the secondary endpoint of PASI 75.[1]**
- **In the BE BRIGHT open label extension study, 62.7% (620/989) of patients achieved PASI 100 at Week 16 (non-responder imputation [NRI]). Of these patients, 84.4% (147/174) of patients randomised to 8 week dosing maintained PASI 100 at Week 148.[2]**

Challenge expectations in psoriasis[1,2]

Discover more

This site contains promotional information on UCB products.

To hear about future UCB projects, educational events and to receive the latest information from UCB, please scan the QR code set your digital preferences.

Use this QR code to access Bimzelx.co.uk

BIMZELX is indicated for the treatment of moderate to severe plaque psoriasis in adults who are candidates for systemic therapy.[1]

Prescribing Information and Adverse Event can be found below.

Note: The most frequently reported adverse reactions with BIMZELX are: upper respiratory tract infections (14.5%) and oral candidiasis (7.3%).[1] Other common adverse events include: Tinea infection, ear infection, Herpes simplex infections, oropharyngeal candidiasis, gastroenteritis, folliculitis, headache, dermatitis and eczema, acne, injection site reaction and fatigue.

PRESCRIBING INFORMATION

(Please consult the Summary of Product Characteristics (SmPC) before prescribing)

BIMZELX® ▼ (Bimekizumab)

Active Ingredient: Bimekizumab – solution for injection in pre-filled syringe or pre-filled pen: *160 mg of bimekizumab in 1 mL of solution (160mg/mL)*. **Indications:** Moderate to severe plaque psoriasis in adults who are candidates for systemic therapy. **Dosage and Administration:** Should be initiated and supervised by a physician experienced in the diagnosis and treatment of plaque psoriasis. **Recommended dose:** 320 mg (given as two subcutaneous injections of 160 mg each) at week 0, 4, 8, 12, 16 and every 8 weeks thereafter. For some patients with a body weight ≥ 120 kg who did not achieve complete skin clearance at week 16, 320 mg every 4 weeks after week 16 may further improve treatment response. Consider discontinuing if no improvement by 16 weeks of treatment. Renal or hepatic impairment: No dose adjustment needed. Elderly: No dose adjustment needed. Administer by subcutaneous injection to thigh, abdomen or upper arm. Rotate injection sites and do not inject into psoriatic plaques or skin that is tender, bruised, erythematous or indurated. Do not shake pre-filled syringe or pre-filled pen. Patients may be trained to self-inject. **Contraindications:** Hypersensitivity to bimekizumab or any excipient; Clinically important active infections (e.g. active tuberculosis). **Warnings and Precautions:** Record name and batch number of administered product. *Infection:* Bimekizumab may increase the risk of infections e.g. upper respiratory tract infections, oral candidiasis. Caution when considering use in patients with a chronic infection or a history of recurrent infection. Must not be initiated if any clinically important active infection until infection resolves or is adequately treated. Advise patients to seek medical advice if signs or symptoms suggestive of an infection occur. If a clinically important infection develops or is not responding to standard therapy, carefully monitor and do not administer bimekizumab until infection resolves. *TB:* Evaluate for TB infection prior to initiating bimekizumab – do not give if active TB. While on bimekizumab, monitor for signs and symptoms of active TB. Consider anti-TB therapy prior to bimekizumab initiation if past history of latent or active TB in whom adequate treatment course cannot be confirmed. *Inflammatory bowel disease:* Bimekizumab is not recommended in patients with inflammatory bowel disease. Cases of new or exacerbations of inflammatory bowel disease have been reported. If inflammatory bowel disease signs/symptoms develop or patient experiences exacerbation of pre-existing inflammatory bowel disease, discontinue bimekizumab and initiate medical management. *Hypersensitivity:* Serious hypersensitivity reactions including anaphylactic reactions have been observed with IL-17 inhibitors. If a serious hypersensitivity reaction occurs, discontinue immediately and treat. *Vaccinations:* Complete all age appropriate immunisations prior to bimekizumab initiation. Do not give live vaccines to bimekizumab patients. Patients may receive inactivated or non-live vaccinations. **Interactions:** A clinically relevant effect on CYP450 substrates with a narrow therapeutic index in which the dose is individually adjusted e.g. warfarin, cannot be excluded. Therapeutic monitoring should be considered. **Fertility, pregnancy and lactation:** Women of child-bearing potential should use an effective method of contraception during treatment and for at least 17 weeks after treatment. Avoid use of bimekizumab during pregnancy and breastfeeding. Discontinue breastfeeding or discontinue bimekizumab during breastfeeding. It is unknown whether bimekizumab is excreted in human milk, hence a risk to the newborn/infant cannot be excluded. No data available on human fertility. **Driving and use of machines:** No or negligible influence on ability to drive and use machines. **Adverse Effects: Refer to SmPC for full information.** Very Common *(≥ 1/10)*: upper respiratory tract infection; Common *(≥ 1/100 to < 1/10):* oral candidiasis, tinea infections, ear infections, herpes simplex infections, oropharyngeal candidiasis, gastroenteritis, folliculitis; headache, dermatitis and eczema, acne, injection site reactions, fatigue; Uncommon *(≥ 1/1,000 to < 1/100):* mucosal and cutaneous candidiasis (including oesophageal candidiasis), conjunctivitis, neutropenia, inflammatory bowel disease. **Storage precautions:** Store in a refrigerator (2°C – 8°C), do not freeze. Keep in outer carton to protect from light. Bimzelx can be kept at up to 25°C for a single period of maximum 25 days with protection from light. Product should be discarded after this period or by the expiry date, whichever occurs first.
Legal Category: POM
Marketing Authorisation Numbers:
Northern Ireland: EU/1/21/1575/002 (2 x 1 Pre-filled Syringes), EU/1/21/1575/006 (2 x 1 Pre-filled Pens) Great Britain: PLGB 00039/0802 (Pre-filled Syringe), PLGB 00039/0803 (Pre-filled Pen). UK NHS Costs: £2,443 per pack of 2 pre-filled syringes or pens of 160 mg each.
Marketing Authorisation Holder: UCB Pharma S.A., Allée de la Recherche 60, B-1070 Brussels, Belgium (Northern Ireland). UCB Pharma Ltd, 208 Bath Road, Slough, Berkshire, SL1 3WE, United Kingdom (Great Britain).
Further information is available from: UCB Pharma Ltd, 208 Bath Road, Slough, Berkshire, SL1 3WE.
Tel: +44 (0)1753 777100 Email: ucbcares.uk@ucb.com
Date of Revision: September 2021 IE-P-BK-PSO-2100102
Bimzelx is a registered trademark.

UK: Adverse events should be reported. Reporting forms and information can be found at www.mhra.gov.uk/yellowcard. Adverse events should also be reported to UCB Pharma Ltd.

References: 1. BIMZELX (bimekizumab) Summary of Product Characteristics. Available from: https://www.medicines.org.uk/emc/product/12834/smpc. Accessed April 2023. **2.** Strober B et al. Poster P1491 presented at the European Academy of Dermatology and Venereology (EADV) meeting, September 7–10 2022; Milan, Italy.

GB-P-BK-PSO-2300114 Date of preparation: April 2023.

Inspired by patients. Driven by science.